Electronic Supporting Information (ESI)

1. Materials and Instrumentations

All general reagents and solvents were purchased from commercial sources. Tetrakis[4-(4-carboxyphenyl)phenyl]ethene (H_4TCPPE) and 1,4-di(1H-imidazol-1-yl)benzene (bib) were prepared according to literature methods.[1,2] The elemental analyses were performed in a PE240C elemental analyzer. The infrared spectra were recorded on a VECTOR 22 spectrometer with pressed KBr pellets. The powder XRD patterns were recorded on a Bruker D8 ADVANCE X-ray diffractometer. Thermal analyses were performed under nitrogen in the temperature range 30–600 ^{o}C with a heating rate of 10 ^{o}C min^{-1} on a TGA-DTA V1.1b Inst 2100 instrument. The sample of activated **1**@nonwoven fabric was prepared in Specac 2T Mini-Pellet Press. Fluorescence spectra were recorded on a Perkin-Elmer LS 55 spectrofluorometer. The fluorescence absolute quantum yields (Φ_{fl}) of the samples were determined with a Horiba Jobin Yvon Fluorolog-3 spectrofluorimeter. Time-resolved fluorescence measurements were performed using a Life-Spec-ps fluorescence lifetime analytical spectrometer (Edinburgh Instruments). Theory calculations were performed using the density functional theory (DFT) with the B3LYP hybrid

2. Crystallographic Studies

Data collection for complexes **1** and **2** were carried out on a Bruker SMART CCD area detector. Hemisphere of data were collected in the θ range of 2.25-21.38 for complex **1** and 2.99-25.00 for complex **2**. The data were integrated using the Siemens SAINT program, with the intensities corrected for Lorentz factor, polarization, air absorption, and absorption due to variation in the path length through the detector faceplate. Empirical absorption and extinction corrections were applied.[3] The structures were solved by direct method and refined on F^2 by full-matrix least squares using SHELXTL.[4] All non-hydrogen atoms were refined anisotropically. All hydrogen atoms were put in calculated positions and refined isotropically with the isotropic vibration parameters related to the non-hydrogen atoms to which they are bonded. The solvent molecules are highly disordered, and the attempt to locate and refine the solvent peaks were unsuccessful. The crystals of **1** and **2** were non-merohedral twin, and the refinement against the intensities was carried out using the Bruker-2004 software package, including the twinning operator.

3. Additional Data

Table S1. Crystal data and structure refinements for complexes **1** and **2**.

Compounds	**1**	**2**
Empirical Formula	$C_{66}H_{42}N_4O_8Zn_2$	$C_{64}H_{40}N_2O_8Zn_2$
Formula weight	1149.78	1095.72
Crystal dimensions [mm]	0.25 × 0.22 × 0.60	0.23×0.21×0.30
Crystal system	Triclinic	Triclinic
Space group	$P\bar{1}$	$P\bar{1}$
a [Å]	15.6667(18)	14.0216(6)
b [Å]	15.8992(18)	16.0891(7)
c [Å]	20.918(2)	20.4898(9)
α [°]	67.16(0)	90.103(2)
β [°]	82.3(0)	99.673(2)
γ [°]	79.75(0)	90.989(2)
V [Å^3]	4713.3(9)	4555.9(3)
Z	2	2
D_c [g cm^{-3}]	0.810129	0.798683
μ [mm^{-1}]	0.545	0.561
F(000)	1180	1124
R_{int}	0.0000	0.0798
T_{max}, T_{min}	21.38, 2.25	25.39，3.03
Goodness-of-fit on F^2	1.194	1.033
R_1, wR_2[a] [$I>2\sigma(I)$]	0.1361, 0.4230	0.0929，0.2528
(all data)	16846	15177
$(\Delta\rho)_{\text{max}}$, $(\Delta\rho)_{\text{min}}$/e Å^{-3}	1.508,-1.141	1.415,-1.272
CCDC no.	1854890	1854891

[a]$R_1 = \Sigma||F_o|-|F_c||/\Sigma|F_o|$; $wR_2=[\Sigma w(F_o^2-F_c^2)^2/\Sigma w(F_o^2)^2]^{1/2}$

Table S2. Selected bond lengths (Å) and angles (°) for complex **1**.

Zn(1)-O(1)	2.110(12)	Zn(2)-O(2)	2.224(10)
Zn(1)-N(1)	2.007(13)	Zn(2)-N(3C)	1.995(13)
Zn(1)-O(3A)	1.956(11)	Zn(2)-O(4A)	1.899(11)
Zn(1)-O(7B)	1.937(12)	Zn(2)-O(8A)	1.898(10)
Zn(1)-O(5D)	2.158(11)	Zn(2)-O(6D)	2.138(11)

O(1)-Zn(1)-N(1)	103.9(5)	O(2)-Zn(2)-N(3C)	95.2(5)
O(1)-Zn(1)-O(3A)	88.4(5)	O(2)-Zn(2)-O(4A)	90.8(4)
O(1)-Zn(1)-O(7B)	87.8(5)	O(2)-Zn(2)-O(8B)	83.0(4)
O(1)-Zn(1)-O(5D)	155.7(5)	O(2)-Zn(2)-O(6D)	163.9(5)
O(3A)-Zn(1)-N(1)	96.3(5)	O(4A)-Zn(2)-N(3C)	108.3(5)
O(7B)-Zn(1)-N(1)	101.1(5)	O(8B)-Zn(2)-N(3C)	100.3(5)
O(5D)-Zn(1)-N(1)	100.3(5)	O(6D)-Zn(2)-N(3C)	100.9(5)
O(3A)-Zn(1)-O(7B)	162.6(6)	O(4A)-Zn(2)-O(8B)	151.2(5)
O(3A)-Zn(1)-O(5D)	86.4(4)	O(4A)-Zn(2)-O(6D)	83.7(4)
O(5D)-Zn(1)-O(7B)	90.1(5)	O(6D)-Zn(2)-O(8B)	94.6(4)

A:x.y,1+z B:1+x,y,z C:x,-1+y,z D:1+x,y,1+z

Table S3. Selected bond lengths (Å) and angles (°) for complex **2**.

Zn(1)-O(1A)	1.990(12)	Zn(2)-O(2A)	2.049(10)
Zn(1)-N(1)	2.014(4)	Zn(2)-N(2A)	2.023(4)
Zn(1)-O(1B)	2.033(12)	Zn(2)-O(2B)	2.106(9)
Zn(1)-O(1C)	1.984(14)	Zn(2)-O(2C)	2.059(11)
Zn(1)-O(1D)	1.994(13)	Zn(2)-O(2D)	2.039(11)
O(1A)-Zn(1)-N(1)	95.6(4)	O(2A)-Zn(2)-N(2)	105.1(4)
O(1A)-Zn(1)-O(1B)	97.0(5)	O(2A)-Zn(2)-O(2B)	88.9(4)
O(1A)-Zn(1)-O(1C)	80.7(5))	O(2A)-Zn(2)-O(2C)	87.8(4)
O(1)-Zn(1)-O(1D)	161.9(5)	O(2A)-Zn(2)-O(2D)	154.3(5)
O(1B)-Zn(1)-N(1)	106.7(3)	O(2B)-Zn(2)-N(2)	96.9(3)
O(1C)-Zn(1)-N(1)	97.5(4)	O(2C)-Zn(2)-N(2)	98.7(4)
O(1D)-Zn(1)-N(1)	100.0(4)	O(2D)-Zn(2)-N(2)	99.2(4)
O(1B)-Zn(1)-O(1C)	155.8(5)	O(2B)-Zn(2)-O(2C)	164.4(4)
O(1B)-Zn(1)-O(1D)	87.3(5)	O(2B)-Zn(2)-O(2D)	96.4(4)
O(1C)-Zn(1)-O(1D)	88.2(6)	O(2C)-Zn(2)-O(2D)	80.3(4)

A:-1+x.y,z B:x,-1+y,-1+z C:x,-1+y,z D:x,y,-1+z

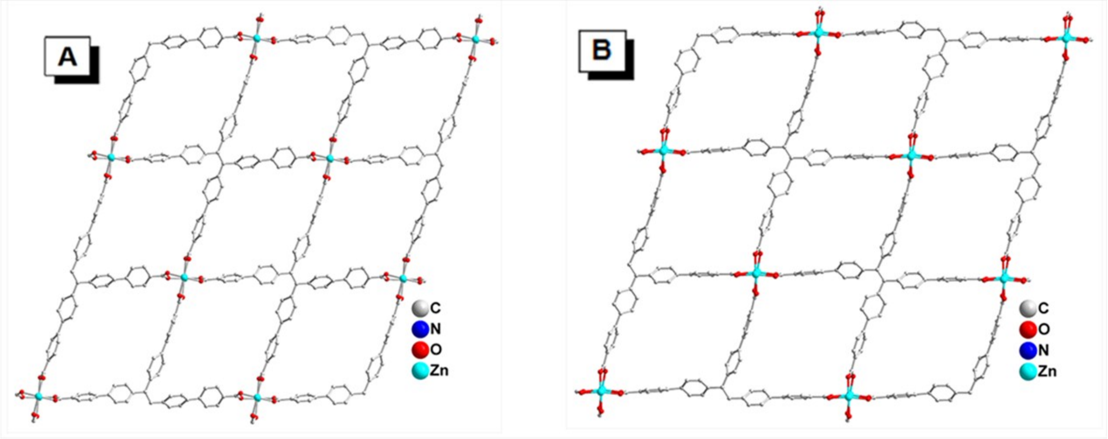

Fig. S1 Two-dimensional grid sheets [Zn_2(TCPPE)] in complexes **1** (A) and **2** (B).

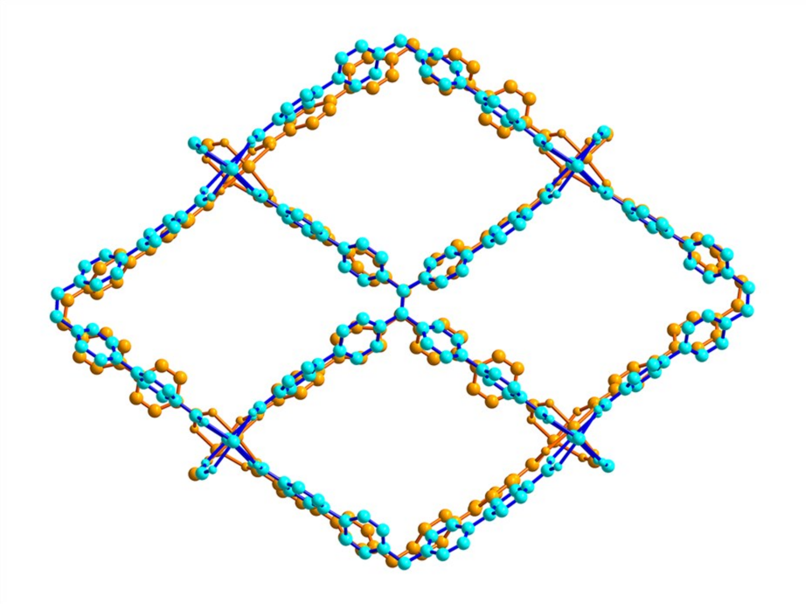

Fig. S2 The overlaid structures of complex **1** (yellow) and complex **2** (blue).

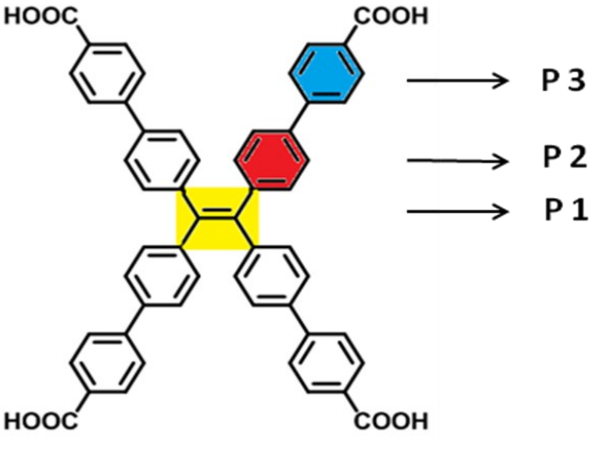

Fig. S3 (A) The plane of the two C atoms forming central C=C double bond and four

C atoms surround them is named P1. The planes crossing phenyl rings attached C=C double bond are named P2. The planes of phenyl rings connected with carboxylic groups are named P3.

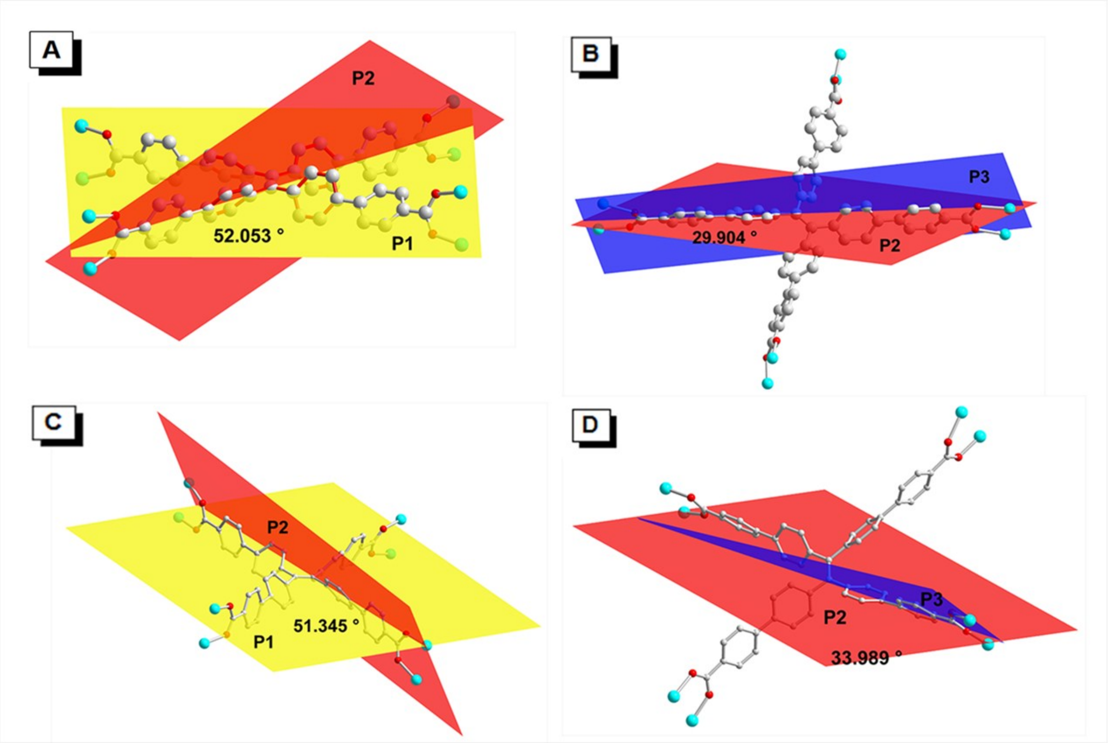

Fig. S4 The average dihedral angles are labeled for (A) P1-P2, (B) P1-P3 in complex **1** and (C) P1-P2, (D) P1-P3 in complex **2**. The average dihedral angles between planes P1 and P2 (<P1-P2) are 52.05º (complex **1**) and 51.345º (complex **2**), which are smaller than those in [Zn_2(TCPPE)] (58.49º) and PCN-94 (55.33º). The average dihedral angles between planes P2 and P3 are 29.90º in complex **1** and 33.989º in complex **2**, which are much smaller than those in [Zn_2(TCPPE)] (47.08º) and PCN-94 (54.45º), and also smaller than that in free ligand (35.93º).[1,5]

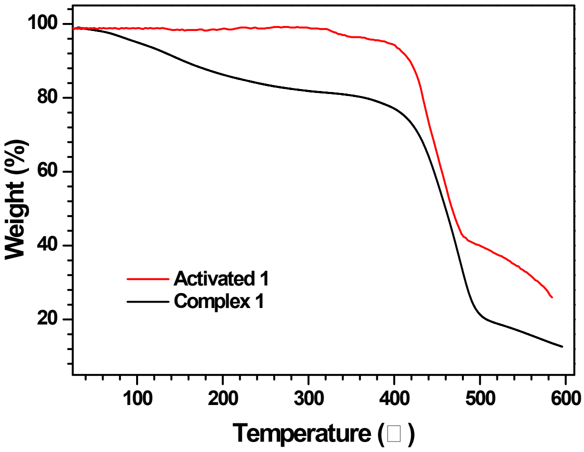

Fig. S5 Thermogravimetric (TG) analyses of complex **1** and activated **1**.

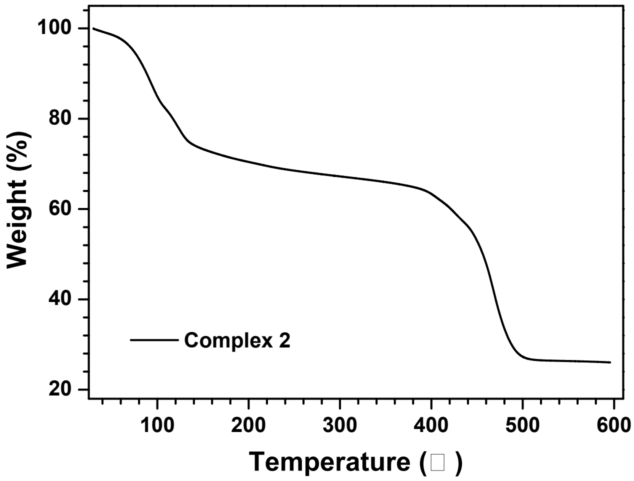

Fig. S6 Thermogravimetric (TG) analyse of complex **2**.

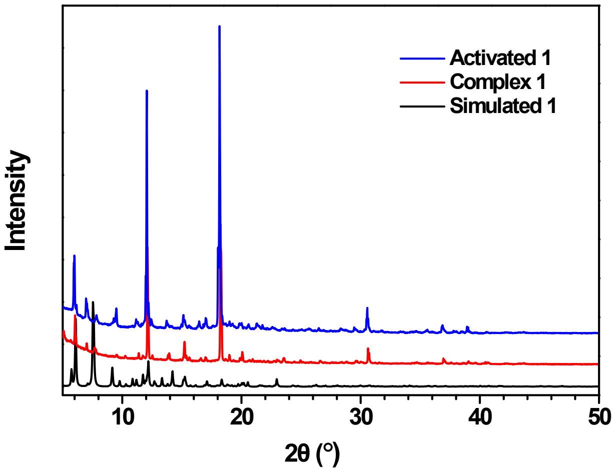

Fig. S7 The PXRD patterns of simulated **1** (black), complex **1** (red) and activated **1** (blue).

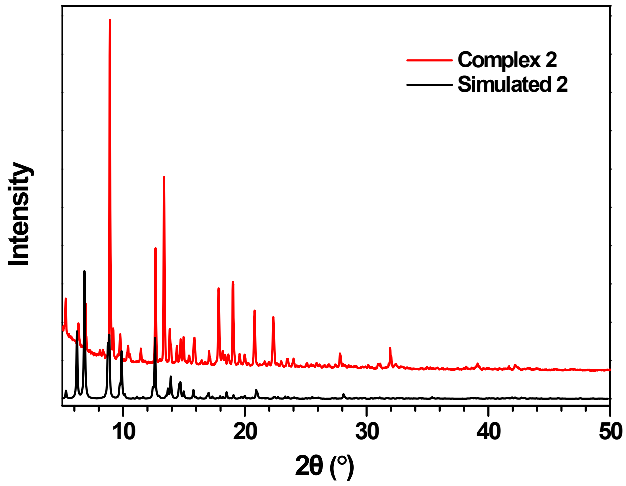

Fig. S8 The PXRD patterns of simulated **2** (black) and complex **2** (red).

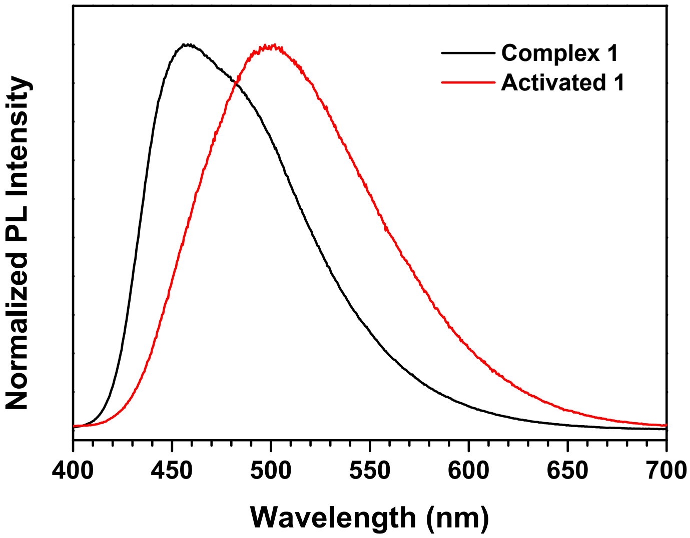

Fig. S9 Solid-state PL spectra of complex **1** and activated **1**.

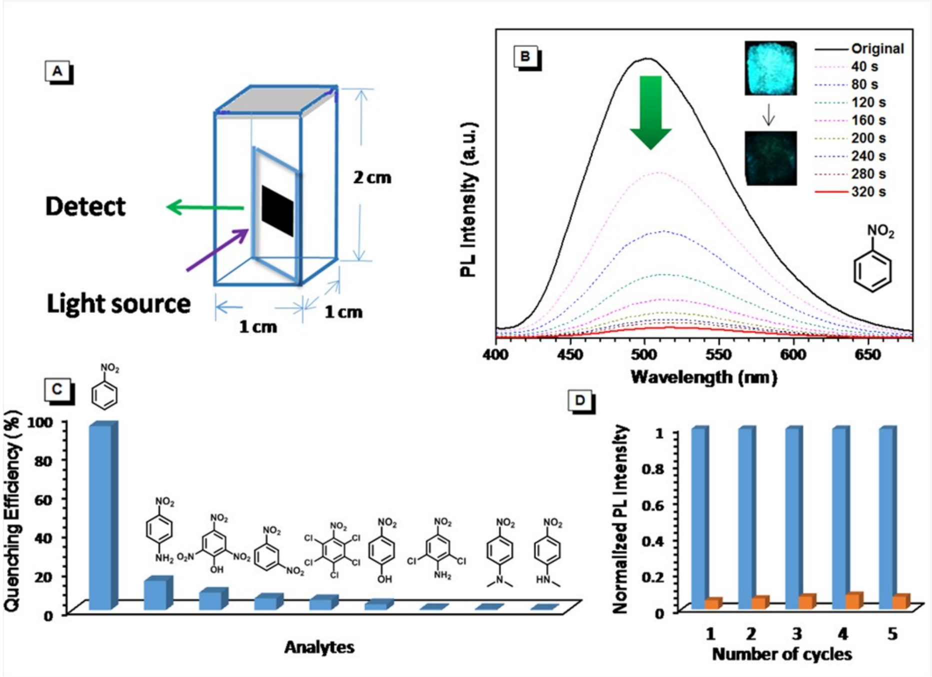

Fig. S10 A) In situ solid-state luminescent sensor setup. B) Emission spectra of activated **1**@nonwoven fabric upon exposure to nitrobenzene vapor at various time intervals at room temperature. Inset: Photos of activated **1**@nonwoven fabric exposure to nitrobenzene vapor (time of 0 and 320 s). C) Fluorescence quenching efficiency after 6 min by nine different analytes at room temperature. D) Five consecutive decrease and regeneration cycles.

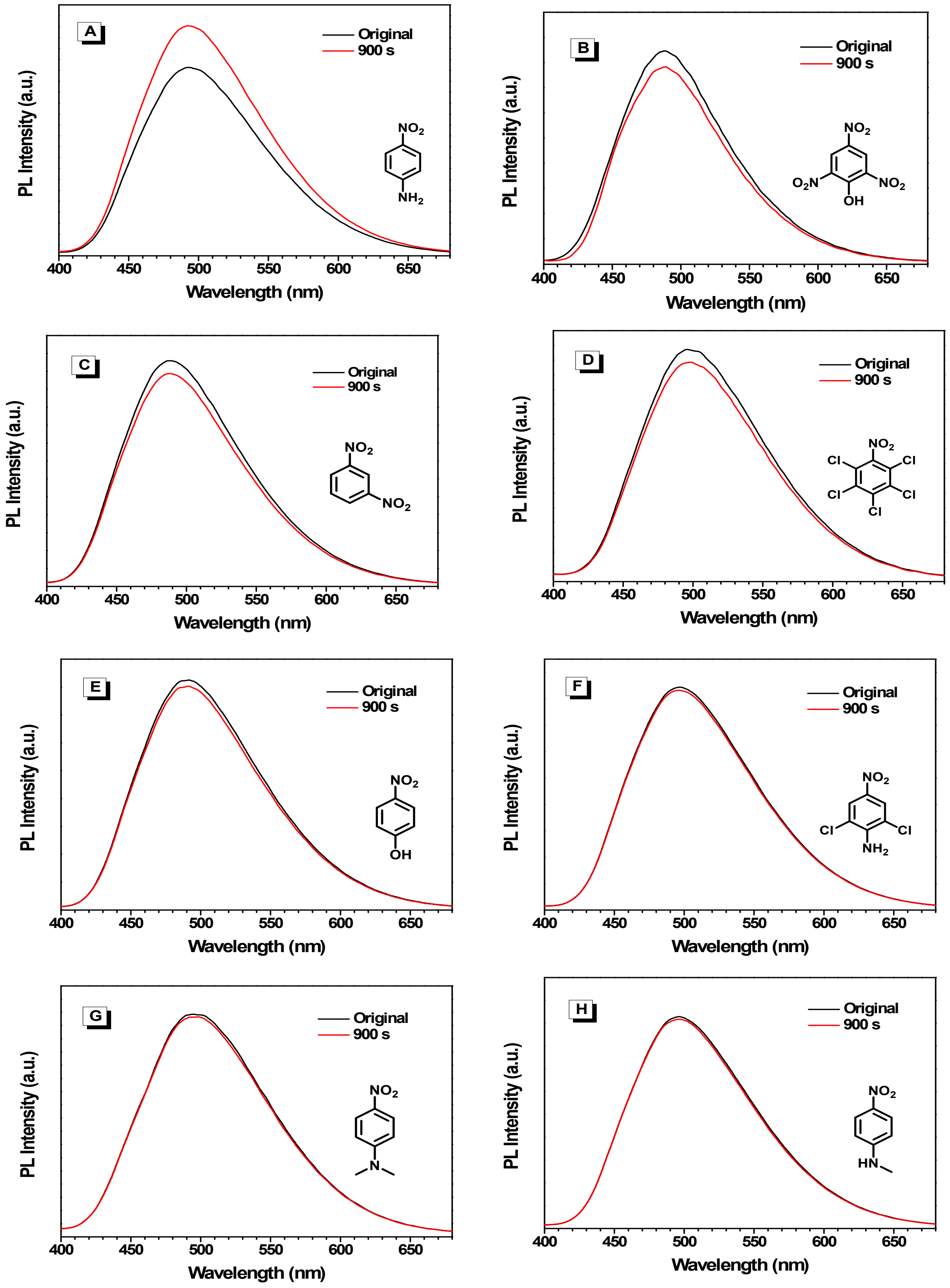

Fig. S11 PL spectra of activated **1**@nonwoven fabric upon exposure to different analyte vapors of 4-nitroaniline, 2,4,6-trinitrophenol, 1,3-dinitrobenzene, 1,2,3,4,5-pentachloro-6-nitrobenzene, 4-nitrophenol, 2,6-dichloro-4-nitroaniline, *N*,*N*-dimethyl-4-nitroaniline, and *N*-methyl-4-nitroaniline.

Table S4. Quenching efficiency of activated **1**@nonwaven faric exposured in different nitro aromatic analyte vapors.

analytes	Quenching efficiency (%)	analytes	Quenching efficiency (%)
4-nitroaniline	15	4-nitrophenol	3
2,4,6-trinitrophenol	9	2,6-dichloro-4-nitroaniline	0.5
1,3-dinitrobenzene	6	N,N-dimethyl-4-nitroaniline	0.5
1,2,3,4,5-pentachloro-6-nitrobenzene	5	N-methyl-4-nitroaniline	0.3

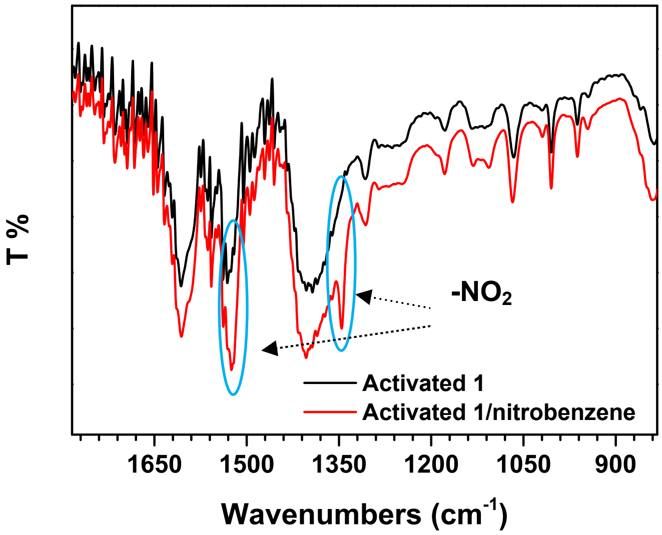

Fig. S12 IR spectra of activated **1** and activated **1** exposured in nitrobenzene vapor.

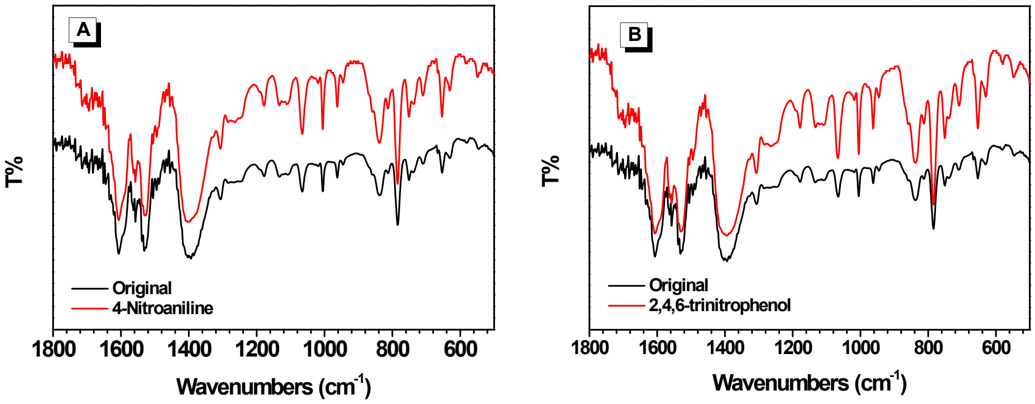

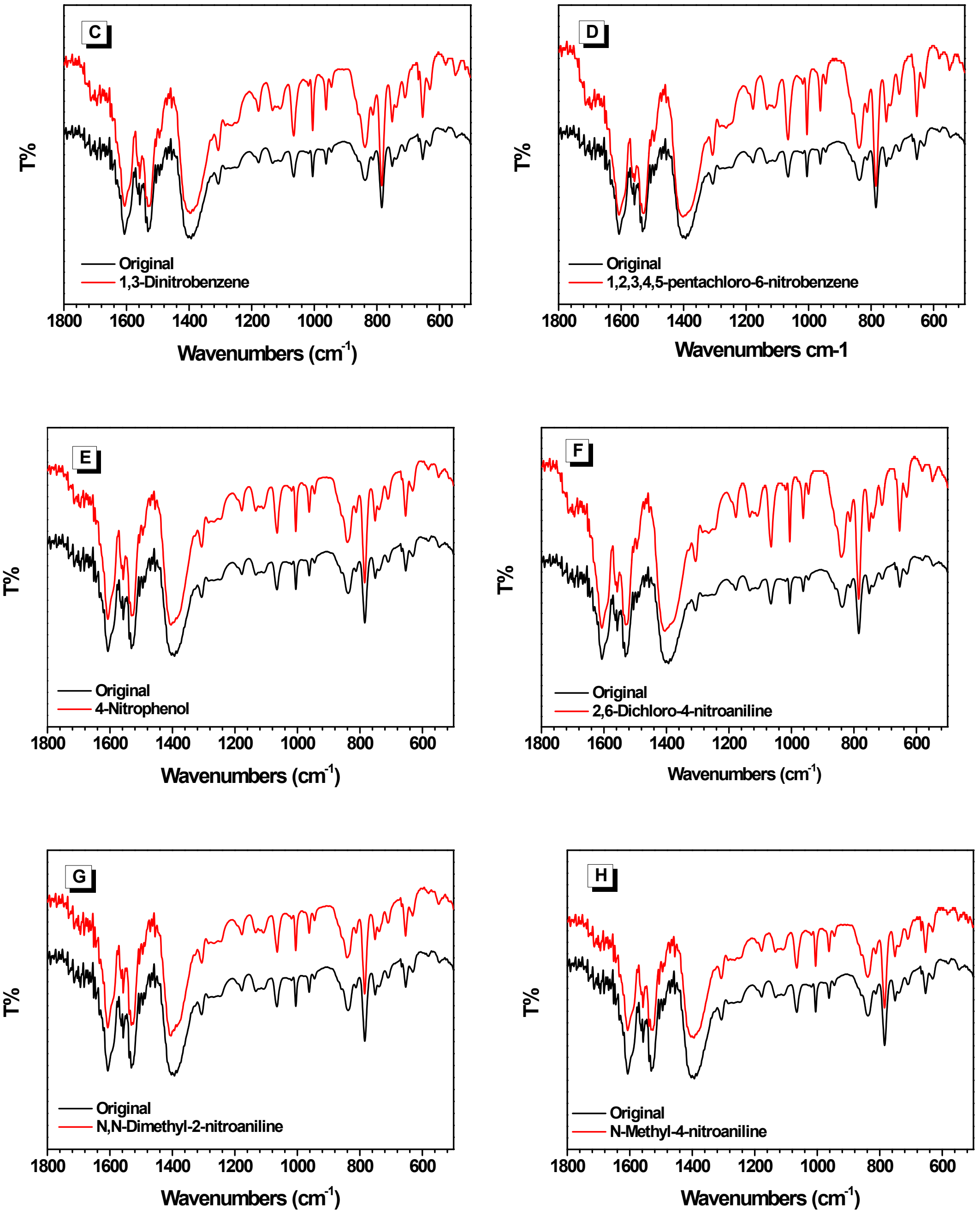

Fig. S13 IR spectra of activated **1** and activated **1** exposured in analyte vapors of 4-nitroaniline (*p*-NPA), 2,4,6-trinitrophenol (TNP), 1,3-dinitrobenzene (*m*-DNB), 1,2,3,4,5-pentachloro-6-nitrobenzene (PCN), 4-nitrophenol (*p*-NPO), 2,6-dichloro-4-nitroaniline (DCNA), *N*,*N*-dimethyl-4-nitroaniline (*p*-DMNPA), and *N*-methyl-4-nitroaniline (*p*-MNPA).

Table S5 The fluorescence lifetimes (τ) **of** activated **1** and that exposed to NB vapors for 40 s, 80 s, 120 s and 360 s.

samples	τ (ns)
0 s	1.96
40 s	1.92
80 s	1.88
120 s	1.88
360 s	1.82

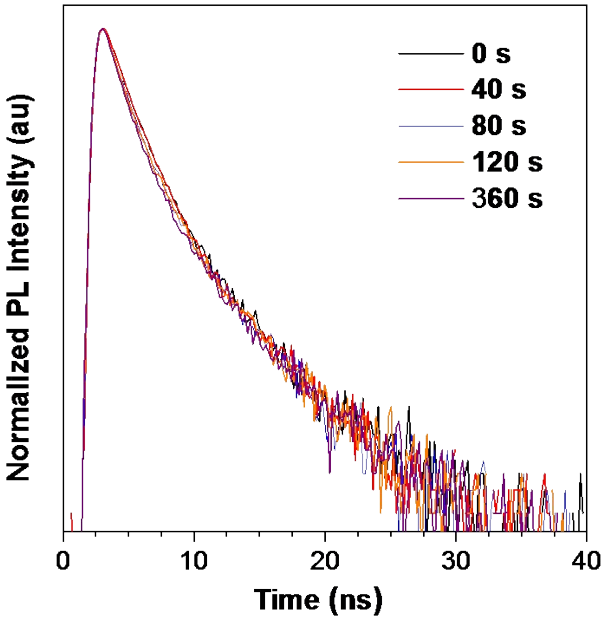

Fig. S14 The fluorescence lifetimes (τ) **of** activated **1** and that exposed to NB vapors for 40 s, 80 s, 120 s and 360 s.

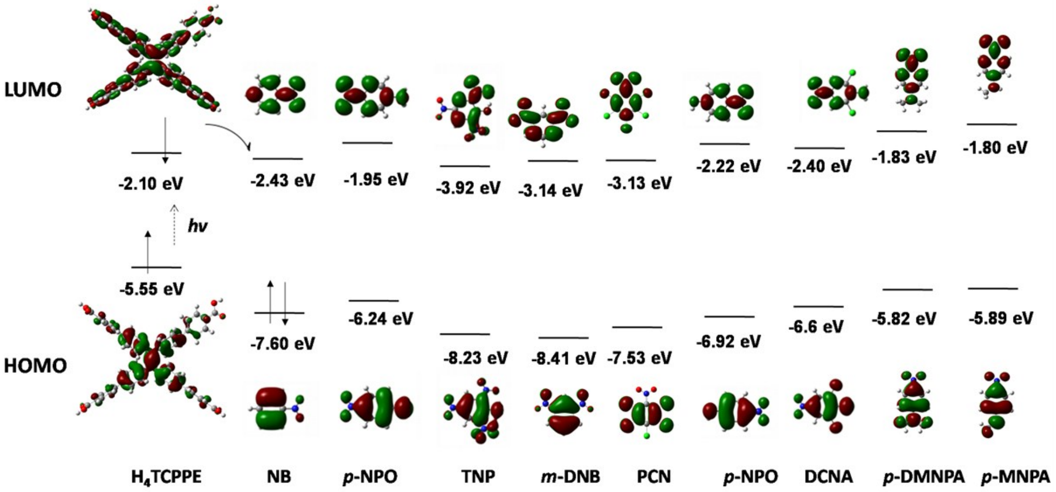

Fig. S15 The HOMO and LUMO energy levels of H$_4$TCPPE in complex **1** and nitro aromatic compounds.

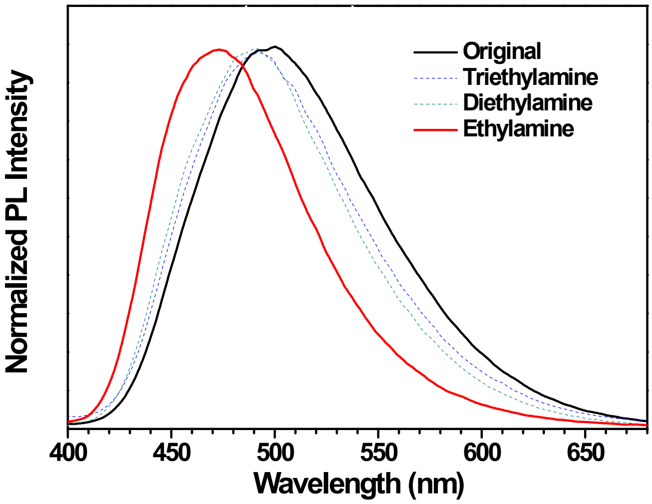

Fig. S16 PL spectra of activated **1**@nonwoven fabric upon exposure to different analyte vapors of triethylamine, diethylamine and ethylamine.

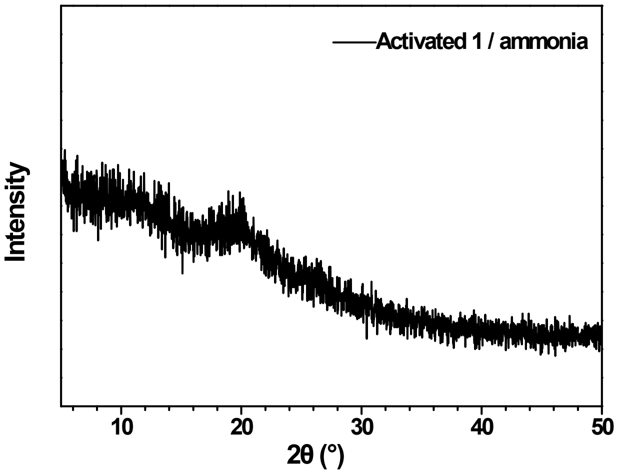

Fig. S17 The PXRD patterns of activated **1** exposured in ammonia.

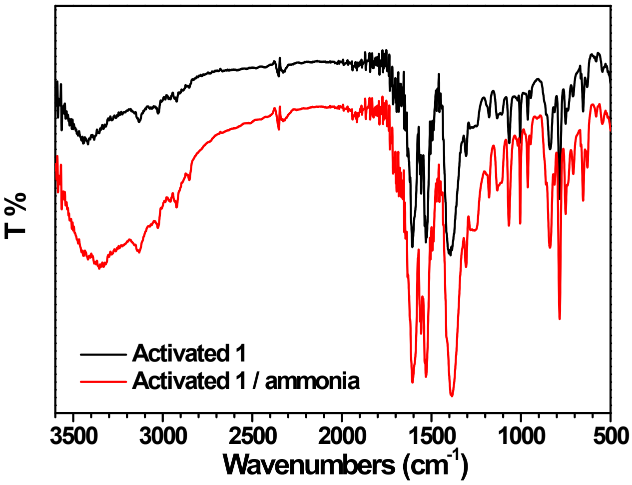

Fig. S18 IR spectra of activated **1** and activated **1** exposured in ammonia.

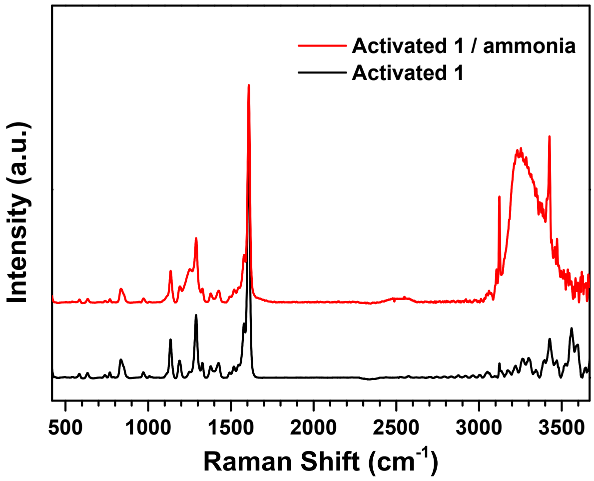

Fig. S19 Raman spectra of activated **1** and activated **1** exposured in ammonia.

4. Reference

1 X.-G. Liu, H. Wang, B. Chen, Y. Zou, Z.-G. Gu, Z. Zhao and L. Shen, *Chem. Commun.*, 2015, **51**, 1677.

2 J. Mao, Q. Hua, J. Guo and D. Shi, *Catal. Commun.*, 2018, **10**, 341.

3 SAINT, Program for Data Extraction and Reduction, Siemens Analytical X-ray Instruments, Madison, WI, 1994–1996.

4 SHELXTL (version 5.0), Reference Manual, SiemensIndustrial Automation, Analytical Instruments, Madison, WI, 1995.

5 Z. Wei, Z.-Y. Gu, K. A. Ravi, Y.-P. Chen, R. N. McDougald, Jr., J. F. Ivy, A. A. Yakovenko, D. Feng, M. A. Omary and H.-C. Zhou, *J. Am. Chem. Soc.* 2014, **136**, 8269.